

Energy Levels of $\text{Tm}^{170}\dagger$

R. K. SHELINE AND C. E. WATSON*

The Florida State University, Tallahassee, Florida

AND

B. P. MAIER, U. GRUBER, R. H. KOCH, AND O. W. B. SCHULT

Physik-Department der Technischen Hochschule München, München, Germany
and
Research Establishment, Risø, Denmark

AND

H. T. MOTZ AND E. T. JURNEY

Los Alamos Scientific Laboratory, University of California, Los Alamos, New Mexico

AND

G. L. STRUBLE

The Florida State University, Tallahassee, Florida
and
The Lawrence Radiation Laboratory, University of California, Berkeley, California

AND

T. V. EGIDY, TH. ELZE, AND E. BIEBER

Physik-Department der Technischen Hochschule München, München, Germany

(Received 11 October 1965)

Twenty-seven levels in Tm^{170} have been observed up to an excitation energy of 1153 keV utilizing 12-MeV deuterons and the reaction $\text{Tm}^{169}(d,p)\text{Tm}^{170}$. The ground-state Q value was determined as 4369 ± 15 keV. Both magnetic Compton and germanium spectrometers have been used to measure 16 high-energy gamma rays up to an excitation energy of 868 keV resulting from the capture of thermal neutrons in the reaction $\text{Tm}^{169}(n,\gamma)\text{Tm}^{170}$. The neutron binding energy observed in this reaction is 6595 ± 2.5 keV. In addition, 177 low-energy gamma rays between 38 and 870 keV have been observed in a bent-crystal spectrograph during irradiation of Tm^{169} with thermal neutrons. The multipolarities of 29 of the transitions were determined from internal conversion measurements with a beta-ray spectrometer. The analysis of these data suggests the existence of 23 levels up to an energy of 720 keV for which assignments have been attempted. Three Nilsson configurations 0, in which the proton orbital Ω_p remains $\frac{1}{2}+[411\downarrow]$ and the neutron orbital Ω_n is successively $\frac{3}{2}-[521\downarrow]$, $\frac{7}{2}+[633\uparrow]$, and $\frac{5}{2}-[512\uparrow]$ 0, account for 16 states. This analysis leads to the following spectroscopic interpretation (band head energy, keV, in parentheses; spin, parity, and K quantum number in brackets): (ground state), $[1-, 1]$ with superimposed band to $4-$; (149.721), $[0-, 0]$ with superimposed band and anomalous spacings of even and odd spin members to $4-$; (183.193), $[3+, 3]$ with superimposed rotational members to $5+$; (204.452), $[2-, 2]$ with superimposed rotational members to $4-$; (447.079), $[3-, 3]$ only member of the band. Seven additional higher energy levels are tentatively assigned, five of which may arise from gamma vibrational bands at 411.45, 661.91, and 719.21 keV built on $K=1-$, $K=0-$ and $K=3+$ intrinsic bands, respectively. These are the first gamma vibrational bands postulated in odd-odd nuclei. All states below 425 keV from both (d,p) and direct high (n,γ) excitation are included in these assignments. The Coriolis coupling between the $K=1-$ and $K=0-$ bands is clearly observed in the anomalous rotational spacing of the $K=1-$ band. Calculation of the energies and (d,p) cross sections for the $K=1-$ and $K=0-$ bands agrees well with experiment and indicates that only the even members of these bands are appreciably mixed. The $M1$ transition probabilities within the $K=0$ rotational band in Tm^{170} are shown to be quite large. It is suggested that the high-energy gamma rays in the reaction $\text{Tm}^{169}(n,\gamma)\text{Tm}^{170}$ involve a direct reaction which excludes population of excited proton configurations.

I. INTRODUCTION

THE odd-odd nucleus Tm^{170} presents some interesting nuclear spectroscopic anomalies. As a deformed nucleus, its 69-proton configuration should be described by the Nilsson orbital $[411\downarrow]\frac{1}{2}+$, whereas the 101-neutron configuration is expected to be described by

the Nilsson orbital $[521\downarrow]\frac{1}{2}-$. Thus, $K=0-$ and $K=1-$ rotational bands are expected from the coupling of the $\frac{1}{2}$ spins of the neutron and proton. The Gallagher-Moszkowski coupling rules¹ suggest that the triplet coupling of the intrinsic spins of the two nucleons is energetically favored. Consequently, the $K=\Omega_p+\Omega_n=1-$ rotation band is expected to be the ground-state rotational band. The ground state of Tm^{170} has indeed

† Work supported by the U. S. and Danish Atomic Energy Commissions.

* The (d,p) reaction spectroscopy was taken from part of the thesis of C. E. Watson presented to Florida State University in April, 1964, in partial fulfillment of the requirements of the Ph.D. degree.

¹ C. J. Gallagher, Jr., and S. A. Moszkowski, Phys. Rev. **111**, 1282 (1958).

been shown experimentally²⁻⁴ to have spin-parity 1^- . The $K=0^-$ rotational band which results from the recoupling of the neutron and proton is normally⁵ split by the neutron-proton residual interaction and the particle-particle coupling⁶ into two bands, one with even spin members, the other with odd spin members.

Thus in Tm^{170} , we have $K=0$ and $K=1$ rotational bands which, since $\Delta K=1$, should be affected by Coriolis coupling. The even-odd splitting should then give rise to anomalous energy spacings in the $K=1^-$ band. On the other hand, the even and odd members of the $K=0^-$ band, which to first order would normally be expected to have very similar moments of inertia, might here be expected to have different moments of inertia due to perturbing effects of the Coriolis coupling. Recent measurements⁷ on the levels in Tm^{172} have shown some anomalies of this type.

The experimental search for these anomalies has been carried on simultaneously in four different laboratories— at Florida State University utilizing the reaction $\text{Tm}^{169}(d,p)\text{Tm}^{170}$, at Los Alamos and Risø using both high- and low-energy gamma spectroscopy for the reaction $\text{Tm}^{169}(n,\gamma)\text{Tm}^{170}$, and at Munich utilizing the conversion electrons from neutron capture on Tm^{169} . Theoretical interpretation has proceeded both at Florida State University and at the University of California.

II. EXPERIMENTAL METHODS AND RESULTS

The skeleton of levels in Tm^{170} on which much of the rest of the level structure hangs resulted initially from (d,p) reaction spectroscopy. For this reason, the (d,p) results will be discussed first. The high-energy (n,γ) results correlate naturally with (d,p) results and are described next. Finally transitions between levels observed in high-resolution low-energy (n,γ) and (n,e) experiments are discussed. These experiments determine the energy of levels much more accurately, define spins and parities, and suggest additional levels.

A. $\text{Tm}^{169}(d,p)\text{Tm}^{170}$

12.0-MeV deuterons from the Florida State University tandem Van de Graaff⁸ have been used to study the reaction $\text{Tm}^{169}(d,p)\text{Tm}^{170}$. The monoenergetic deuteron beam was focused through a series of slits, colli-

ating it to a $\frac{1}{4}$ by 3-mm spot on the target which served as a line source for the magnetic spectrograph. Beam currents on the target varied from 0.25 to 1.0 μA . Targets of the naturally occurring 100% abundant Tm^{169} obtained from the Lindsay Corporation were prepared in the following manner. Carbon was deposited on glass microscope slides which had previously been coated with a thin layer of Teepol. This disposition was accomplished utilizing spectroscopically pure carbon vacuum evaporated into thin layers of carbon 15–30 $\mu\text{g}/\text{cm}^2$ thick. The 100% Tm^{169} was then evaporated as metal onto the carbon backing by electron bombardment of a carbon crucible containing the metal. The carbon film containing the metallic Tm^{169} target was floated off in ion-exchanged water and picked up on an aluminum frame designed to fit the target chamber. The metallic Tm targets were estimated to be 200–300 $\mu\text{g}/\text{cm}^2$ thick. Protons emitted from the (d,p) reaction were analyzed using a modified 6/5 scale up of the Browne-Buechner broad range magnetic spectrograph. Complete details of this spectrograph are contained elsewhere.^{9,10} Emergent proton groups were collimated by a slit system and bent toward an array of four 2-in. \times 10-in. 50 μ Eastman NTA nuclear track plates. The plates were arranged end-to-end and spring fitted against the focal curve of the magnet. They were covered with 5-mil aluminum foil to stop the deuterons. This simplified the tedious job of plate counting, particularly at the forward angles. Use of this foil does not measurably affect the resolution of the spectrograph for protons. The data presented here are given as the number of proton tracks per half-millimeter strip of plate as a function of the distance along the plate array. The data were analyzed using the Florida State University 709 computer with the application of a least-squares curve fitting program. This program determines the centroids of the proton groups, and at the same time determines the uncertainty in the centroid assignment. With this treatment of the data, although the resolution of the spectrograph is approximately 12 keV, it is usually possible to obtain energy differences between peaks, of a fraction of a keV in favorable cases and generally of the order of 1 keV. In spite of the good statistics of the ground-state proton group which would suggest an uncertainty of approximately 0.5 keV, the Q value of the ground state is systematically low relative to the ground-state Q value derived from the other low-lying proton groups. We have no explanation for the fact that this systematic departure occurs. Therefore, the ground-state Q value quoted at the conclusion of this section is the sum of the measured Q values to the 149.721-keV state and 149.7-keV rather than the directly measured Q value to the ground state.

The proton fits resulting from the reaction $\text{Tm}^{169}(d,p)$ -

² I. Lindgren, A. Cabezas, and W. Nierenberg, *Bull. Am. Phys. Soc.* **5**, 273 (1960).

³ R. L. Graham, J. L. Wolfson, and R. E. Bell, *Can. J. Phys.* **30**, 459 (1952).

⁴ C. J. Gallagher and V. G. Soloviev, *Kgl. Danske Videnskab. Selskab Mat. Fys. Skrifter* **2**, No. 2 (1962).

⁵ F. Asaro, I. Perlman, J. O. Rasmussen, and S. G. Thompson, *Phys. Rev.* **120**, 934 (1960).

⁶ N. D. Newby, Jr., *Phys. Rev.* **125**, 2063 (1962).

⁷ P. G. Hansen, H. L. Nielsen, E. T. Williams, K. Wilsky, and G. Sidenius, *Comptes Rend. Congr. Intern. Phys. Nucl.* **3b(II)/C79**, 538, 1964 (unpublished).

⁸ The operation of the Florida State University Tandem Van de Graaff has been facilitated through support of the Office of Scientific Research of the U. S. Air Force and the Nuclear Program of the State of Florida.

⁹ R. A. Kenefick and W. N. Shelton, theses submitted to Florida State University, 1962 (unpublished).

¹⁰ C. P. Browne and W. W. Buechner, *Rev. Sci. Instr.* **27**, 899 (1956).

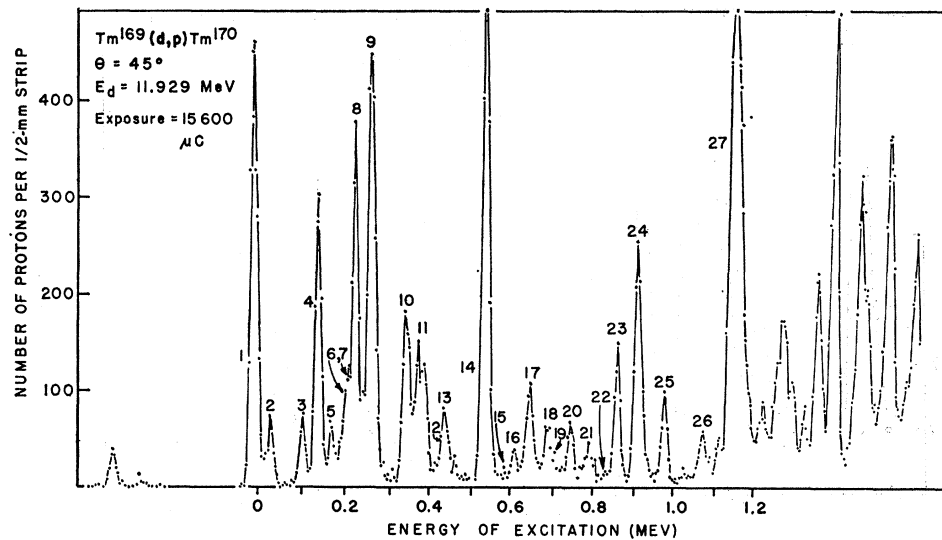


FIG. 1. Proton spectrum from the reaction $Tm^{169}(d,p)Tm^{170}$ observed at a laboratory angle of 45° .

Tm^{170} were analyzed in 5° steps from 10° to 45° , and in 10° steps from 45° to 135° . Typical data taken at 45° are shown in Fig. 1. An average of the 17 runs for the level energies observed in Tm^{170} is shown in Table I.

Using the cross sections measured at the different angles normalized by inelastic deuteron scattering, angular distributions were determined. The results of the

intensities plotted versus angle are shown in Fig. 2 together with distorted wave Born approximation (DWBA) calculations utilizing the JULIE code with the optical-model parameters previously successfully used for the $Yb^{176}(d,p)Yb^{177}$ reaction. The assigned angular momentum transfers are not unique. Often, in fact, two or more different angular distributions will fit within the experimental error. Fortunately, the Nilsson orbitals and the amount of Coriolis coupling involved determine uniquely the cross sections for particular rotational members of the bands. The angular distributions presented here are in complete agreement with the spins

TABLE I. Energy levels and Q values for the reaction $Tm^{169}(d,p)Tm^{170}$.

Level number	Q value (keV)	Excitation energy (keV) ^a
1	4366.6 ^b	+2.5(G.S.) \pm 3.0
2	4329.6	39.5 \pm 1.2
3	4254.1	115.0 \pm 1.2
4	4219.5	149.6 \pm 0.6
5	4185.8	183.3 \pm 1.1
6	4160.9	208.2 \pm 1.7 ^c
7	4150.9	218.2 \pm 2.4 ^c
8	4132.5	236.6 \pm 0.6
9	4099.5	269.6 \pm 0.5
10	4015.9	353.2 ^d
11	3988.7	380.4
12	3941.8	427.3
13	3922.9	446.2
14	3827.0	542.1
15	(3781.3)	(587.8) ^e
16	3759.2	609.9
17	3718.9	650.2
18	3679.5	689.6
19	3651.2	717.9
20	3615.2	753.9
21	3582.1	787.0
22	(3527.7)	(841.4) ^e
23	3502.9	865.2
24	3453.4	915.7
25	3383.3	985.8
26	3299.9	1069.2
27	3216.2	1152.9

^a Errors quoted are twice the standard deviations obtained from the fitting program. They include no systematic errors.

^b Correct ground state Q value is 4369 ± 15 keV (see text).

^c For the 45° run only.

^d Errors are not statistically determined from this excitation energy to higher excitations. Reasonable errors are 1.0–4.0 keV.

^e Level doubtful.

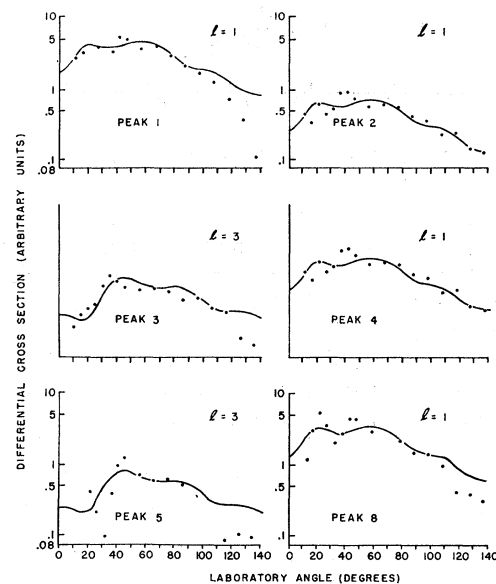


FIG. 2. Angular distributions of six of the first eight groups observed in Fig. 1. Peak numbers refer to the labels in Fig. 1. Dots are experimental points. The solid lines are the theoretical angular distributions (see text) for angular-momentum transfers indicated in each of the six distributions.

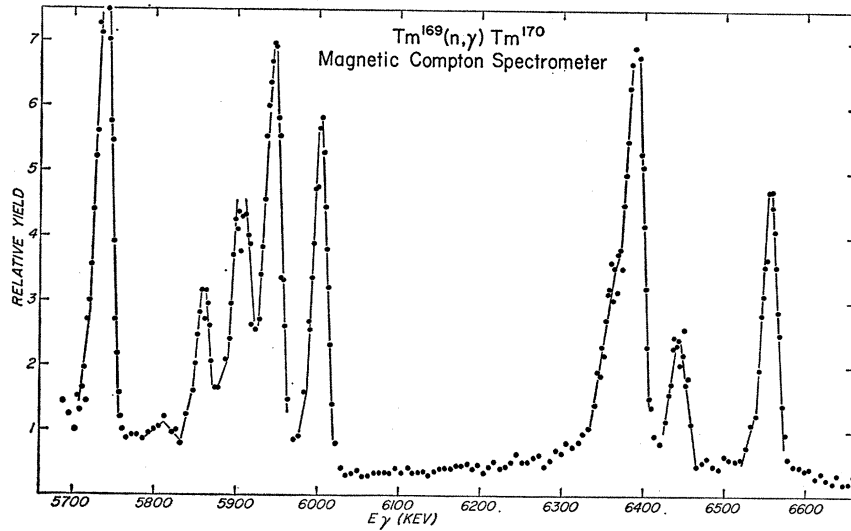


FIG. 3. High-energy $Tm^{169}(n,\gamma)-Tm^{170}$ spectrum from the Los Alamos magnetic Compton spectrometer.

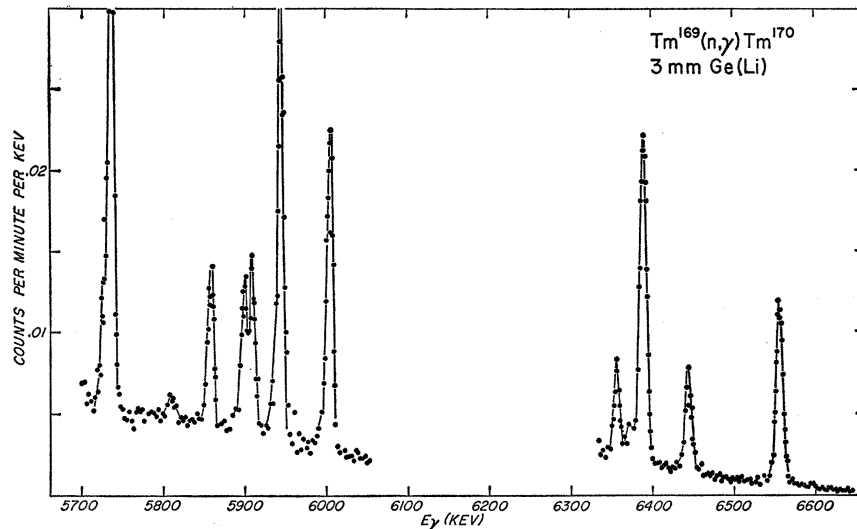


FIG. 4. High-energy $Tm^{169}(n,\gamma)-Tm^{170}$ spectrum obtained at Los Alamos with a 3-mm deep Li-drifted germanium detector. Running time was 3070 min.

and parities assigned to the states utilizing the cross sections in this way.

The reaction $C^{12}(d,p)C^{13}$ with the known Q value 2.7224 ± 0.0005 keV was taken as a reference to infer the incident energy of the deuteron beam. Using this as a calibration, the ground-state Q value for the reaction $Tm^{169}(d,p)Tm^{170}$ is 4369 ± 15 keV.

The comparison of data from the (d,p) reaction with the high- and low-energy gamma-ray spectra and conversion electrons from the (n,γ) reaction are presented in Sec. III. Interpretation of the observed levels in terms of rotational bands built on the appropriate Nilsson intrinsic states will also be considered in this section.

B. High-Energy (n,γ) Spectra

Figure 3 shows a portion of the high-energy spectrum from $Tm^{169}(n,\gamma)$ as determined by the Los Alamos magnetic Compton spectrometer.¹¹ This is a double-

focusing instrument with $\rho_0 = 35$ cm having four electron detectors combined with two back-scattered gamma detectors to provide for eight simultaneous counting channels. In this experiment, the target was 90 g of Tm_2O_3 placed in the thermal column of the Omega West reactor.

A computer code is used to apply a least-squares fit of the spectrometer data to a skewed Gaussian function.¹¹ Both the skewness and width have been determined carefully over a large energy range for strong single γ rays from various targets. Since the non-linearity of the spectrometer is less than 2 keV over the energy range of 2.5 to 11 MeV,¹² the major error in measuring energy differences over a range of several hundred kilovolts is the statistical error in determining line energies. The absolute uncertainty in energy around 6 MeV is 2.5 keV, which should be combined with the

¹¹ H. Motz and G. Bäckström, *Alpha, Beta and Gamma-Ray Spectroscopy*, edited by Kai Siegbahn (North-Holland Publishing Company, New York, 1965), Chap. XIII, Vol. I.

¹² R. E. Carter and H. Motz, International Conference on Nuclear Physics with Reactor Neutrons, Argonne National Laboratory Report No. ANL 6797, 1963, p. 179 (unpublished).

TABLE II. Tm^{170} high-energy capture gamma rays.

Compton spectrometer		Germanium spectrometer		"Best" value	
E_γ (keV)	I_{rel}	E_γ (keV)	I_γ ($\gamma/10^3n$)	E_γ (keV)	I_γ ($\gamma/10^3n$)
(6587.5 \pm 4) ^a	3 \pm 1	(6594.5 \pm 4) ^a	0.14 \pm 0.04	(6591 \pm 4) ^a	0.14 \pm 0.04
6556.4 \pm 0.5	56 \pm 2	6556.4 ^b	4.6 \pm 0.90	6556.4 \pm 0.5	4.6 \pm 0.90
6444.2 \pm 1	29 \pm 2	6444 \pm 2	2.2 \pm 0.45	6444.2 \pm 1	2.2 \pm 0.45
6395 \pm 2	100 \pm 5	6389 \pm 2	8.0 \pm 1.6	6389 \pm 2	8.0 \pm 1.6
6384 \pm 3		6376 \pm 4	0.79 \pm 0.16	6376 \pm 4	0.79 \pm 0.16
6359 \pm 1.5	28 \pm 2	6356 \pm 2	2.2 \pm 0.45	6356 \pm 2	2.2 \pm 0.45
6003.8 \pm 0.5	67 \pm 5	6004 \pm 2	6.2 \pm 1.3	6003.8 \pm 0.5	6.2 \pm 1.3
5945.0 \pm 0.5	86 \pm 5	5945 ^b	7.9 \pm 1.6	5945.0 \pm 0.5	7.9 \pm 1.6
5906.4 \pm 1	51 \pm 2	5910 \pm 3	2.9 \pm 0.6	5910 \pm 3	2.9 \pm 0.6
		5900 \pm 3	2.6 \pm 0.55	5900 \pm 3	2.6 \pm 0.55
5860.9 \pm 1	26 \pm 2	5859 \pm 2	2.9 \pm 0.60	5860.9 \pm 1	2.9 \pm 0.60
5807 \pm 3	6 \pm 2	5810 \pm 4	0.5 \pm 0.15	5807 \pm 3	0.5 \pm 0.15
5738.6 \pm 0.5	106 \pm 5	5737 \pm 2	8.2 \pm 1.6	5737 \pm 2	8.2 \pm 1.6
		5727 \pm 2	1.4 \pm 0.35	5727 \pm 2	1.4 \pm 0.35

^a Ground state transition. This line is weak in both spectra and should be considered doubtful.

^b Compton spectrometer value used to adjust germanium energy scale.

relative errors given in Table II to give the absolute energy errors.

Figure 4 shows the same part of the Tm spectrum obtained with a Li-drifted germanium detector operated as a 2-quantum escape spectrometer. In this arrangement, 4.6 g of Tm_2O_3 target material was put at the center of a 9- \times 9-cm Bi pipe placed laterally through the reactor thermal column.¹³ One end of the pipe ends in the reactor shield, and the other joins to a collimator carefully aligned to produce a gamma-ray beam \sim 1 cm in diameter at the detector. The detector is located \sim 6 m from the target and by additional collimation views only the target. The 1.5-cm diam. by 3-mm-deep detector is operated inside a NaI annulus 30 cm long with a 20-cm outside diameter and 6.5-cm bore. Pulses from the Ge detector are stored in a 400-channel analyzer only when the annulus gives a coincident pulse at 1022 keV \pm 10%. The large solid angle and thickness of the annulus results in a high (\sim 60%) efficiency for the double-escape peak, but unfortunately Compton events can also give annulus pulses falling within the gating range which contribute to the background. In spite of this effect, the ratio of peak height to background is improved by about a factor of 3 by using the 2-quantum escape mode of operation.

Computer least-squares fitting is also applied to data from the germanium spectrometer. The fitted function is of the form

$$Y(E) = \frac{A}{\sigma(2\pi)^{1/2}} \exp\left(\frac{-x^2}{2\sigma^2}\right) + CA \exp(-Dx) \left[1 - \exp\left(\frac{-x^2 G^2}{2}\right)\right] + \text{const.}$$

Each line fitted has five associated parameters, any of which can be allowed to vary or can be arbitrarily held constant: σ , the linewidth; A , the integrated line in-

tensity; $E_0 = (E-x)$, the position of the line centroid; C , the extrapolated height of an exponential tail at the Gaussian peak; and D , the exponential slope of the tail. Thus, for example, if convergence is obtained with a larger width than expected for a given peak, a doublet with fixed widths can be attempted.

The energy scale for the lines obtained with the Ge detector shown in Table II was fixed by the 6556.4- and the 5945-keV lines as determined from the Compton spectrometer. The improved resolution [8.5 versus 23-keV full width at half-maximum (FWHM)] of the Ge detector over the Compton spectrometer, which is clearly shown in the comparison between Figs. 3 and 4, made it possible to resolve close-lying transitions: for instance, the lines between 6356 and 6389 keV, and the doublet at 5900 and 5910 keV. Except where additional structure is observed, the energy errors on the Ge values must be greater than those on the Compton spectrometer determination.

C. Comparison of High Energy (n,γ) and (d,p) Results

If it is assumed that the highest energy gamma rays arise from the capturing state in Tm^{170} , then these gamma rays define levels in the low-energy excitation region of Tm^{170} which can be compared with the levels experimentally observed in the $Tm^{169}(d,p)Tm^{170}$ reaction. This comparison is made in Table III and is shown graphically in Fig. 5. It is worthy of note that all levels defined by the high-energy (n,γ) experiments have a counterpart in the (d,p) experiments up to an excitation energy of 734 keV. The (d,p) level at 689.6 \pm 2 keV appears from a close inspection of the data to be abnormally wide and undoubtedly corresponds to the (n,γ) doublet at 685 \pm 3 and 695 \pm 3 keV. The most curious feature of the (n,γ) results is the lack of a strong $E1$ transition to the 1- ground state.

The neutron binding energy of Tm^{170} , 6595.1 \pm 2.5 keV, computed by summing the energies of the 38.7-keV state and the 6556.4-keV gamma ray populating it, corresponds well with the sum, 6594 keV, of the (d,p)

¹³ E. T. Jurney and H. Motz, International Conference on Nuclear Physics with Reactor Neutrons, Argonne National Laboratory Report No. ANL 6797, 1963, p. 236 (unpublished).

TABLE III. Levels in Tm¹⁷⁰ from (*n,γ*) and (*d,p*) reactions. [Only levels which depopulate directly to the ground state are listed under low-energy (*n,γ*)].

Low-energy (<i>n,γ</i>)		High-energy (<i>n,γ</i>)		<i>(d,p)</i>	
<i>E</i> (keV)	<i>I_γ</i> /100 <i>n</i>	<i>E</i> (keV)	<i>I_{rel}</i>	<i>E</i> (keV)	<i>I_{rel}</i> (45°)
38.713±0.002	0.17±0.017	(4±4)	2±1	2.5±(3.0)	5.25±0.6
114.543±0.004	3.25±0.33	38.7±0.5	57±3	39.5± 1.2	0.8 ±0.2
149.721±0.003	5.9 ±0.6			115.0± 1.2	0.8 ±0.2
		150.9±1	27±2	149.6± 0.6	3.6 ±0.5
204.452±0.004	9.2 ±0.9	206 ±2	100±5	183.3± 1.1	0.8 ±0.2
219.713±0.017	2.8 ±0.3	219 ±4	11±2	208.2± 1.7	0.6 ±0.3
237.246±0.012	3.9 ±0.4	239 ±2	27±2	218.2± 2.4	0.7 ±0.3
				236.6± 0.6	4.5 ±0.5
				269.6± 0.5	5.8 ±0.6
				353.2	1.9 ±0.3
				380.4	1.3 ±0.2
411.45 ±0.04	2.7 ±0.3			427.3	0.4 ±0.2
				446.2	0.8 ±0.2
456.0 ±0.3	0.9 ±0.14				
512.35 ±0.1	2.4 ±0.2				
537.94 ±0.4	0.8 ±0.16			542.1	6.2 ±0.7
		591.3±0.5	56±10	(587.8)	0.2 ±0.1
604.08 ±0.15	1.7 ±0.017			609.9	0.4 ±0.1
		650.1±0.5	74±12	650.2	1.2 ±0.2
		685 ±3	24±3		
		695 ±3	23±3	689.6	0.7 ±0.2
719.21 ±0.06	1.3 ±0.26			717.9	0.4 ±0.2
		734.2±1	24±2		
		788 ±3	5±2	753.4	0.8 ±0.2
				787.0	0.6 ±0.2

ground-state *Q* value, 4369±15 keV, and the deuteron binding energy, 2225 keV.

With the usual assumption that only *s* capture of reactor neutrons occurs in the reaction Tm¹⁶⁹(*n,γ*)-Tm¹⁷⁰, it seems certain that the capturing state(s) in Tm¹⁷⁰ must have spin-parity 1+ or 0+ and 1+. The close correlation between the (*d,p*) excited states (which can involve only excited neutron configurations) and the (*n,γ*) excited states is discussed in Sec. IV F.

D. Low-Energy (*n,γ*) and (*n, e⁻*) Studies

Since the low-energy neutron capture gamma rays and the internal conversion coefficients of these gamma rays are naturally considered together, the experimental procedures and results are also presented together. The bent-crystal gamma spectrometer at the DR-3 Risø reactor was used to study the neutron-capture gamma rays from the reaction Tm¹⁶⁹(*n,γ*)Tm¹⁷⁰. The instrument¹⁴ and also method of measurement¹⁵ have recently been described. The source for this experiment consisted of 54 mg of Tm¹⁶⁹ as the compound Tm₂O₃. For thermal neutrons the cross section is $\sigma_{th}=130$ b. An average linewidth of 9 sec of arc permitted a resolution of 0.055% for a 100-keV line in the third order and 0.33% for a 600 keV in the second-order reflection. Typical data are shown in Figs. 9 and 10.

¹⁴ U. Gruber, B. P. Maier, and O. W. B. Schult, *Kerntechnik* **5**, 17 (1963); B. P. Maier, U. Gruber, and O. W. B. Schult, *ibid.* **5**, 19 (1963).

¹⁵ O. W. B. Schult, U. Gruber, B. P. Maier, and F. Stanek, *Z. Physik* **180**, 298 (1964).

The beta spectrometer at the FRM Garching reactor used to measure the conversion electron spectrum has also been described recently.^{16,17} This instrument is now better aligned and the magnetic field stabilized and adjusted to an accuracy of 5×10^{-5} by means of a rotating coil.¹⁸ At low energies the background was reduced to $\sim \frac{1}{3}$ by placing a 3.5-cm Bi metal shield between the evacuated tube where the source is installed and the reactor core.¹⁹ The 85- \times 9-mm metallic target of Tm¹⁶⁹ produced by evaporation had a thickness of 0.4 mg/cm². The linewidth at half-maximum was 0.25% at 250 keV due largely to the thickness of the target. Between 1 and 800 keV, 3800 counts of 1 min each were made.

Table IV lists 177 gamma lines between 38 and 870 keV observed in the reaction Tm¹⁶⁹(*n,γ*)Tm¹⁷⁰. Column I gives their relative energies determined with respect to the absolute energies of the *K_{α1}* and *K_{α2}* x rays of Tm as given by Bergvall.²⁰ $|E_{rel}/E_{abs}(\text{keV})-1|$ is less than 4×10^{-5} . The energy errors in Column II are also relative. They are calculated with respect to the precision of the spectrometer and the angular measurements and do not include uncertainties in the conversion factors used in converting wavelength to energy. The intensities in Column III (given as photons/100 captures) were

¹⁶ T. v. Egidy, *Ann. Phys.* **9**, 221 (1962).

¹⁷ E. Bieber, T. von Egidy, and O. W. B. Schult, *Z. Physik* **170**, 465 (1962).

¹⁸ W. Norenberg, Diplomarbeit TH Munchen, 1963 (unpublished); also in *Z. Angew. Phys.* (to be published).

¹⁹ H. Lawin, Diplomarbeit, TH, Munchen, 1964 (unpublished).

²⁰ P. Bergvall, *Arkiv Fysik* **16**, 57 (1960).

TABLE IV. Low-energy gamma rays and electrons emitted during the reactions $Tm^{168}(\alpha, \gamma)Tm^{170}$ and $Tm^{168}(\alpha, e^-)Tm^{170}$. Column I labeled $E_{\gamma, \text{rel}}$ is the relative energy of the gamma ray in keV with respect to the $K_{\alpha 1}$ and $K_{\alpha 2}$ x rays of Tm; Column II labeled $\Delta E_{\gamma, \text{rel}}$ is the relative error in the energy excluding uncertainties in the conversion coefficients; Column III labeled $I_{\gamma}/100c$ is the intensity in photons per 100 neutrons captured; Column IV labeled ΔI_{γ} is the uncertainty in the photon intensity in percent; Column V labeled remark indicates that the gamma has been utilized in the decay scheme if a check appears, indicates more than one gamma ray is present if the word "Compl." is used and indicates the presence of a radioactive nuclide producing the gamma ray by identifying the radioactive nuclide, e.g., Yb^{170} , Tm^{170} ; Column VI labeled electron shell gives the shell(s) in which internal conversion has occurred; Column VII labeled E_e (keV) gives the energy of the conversion electron in keV; Column VIII labeled $I_e/100c$ gives the intensity of internal conversion electrons per 100 neutrons captured; Column IX labeled dI_e/I_e is the uncertainty in the internal conversion electron intensity in percent; Column X labeled I_e/I_{γ} is the measured internal conversion coefficient; Column XI labeled theoretical conversion coefficient of Sliv and Band gives these values for $E1$, $E2$, and $M1$ multipolarity; Column XII labeled multiple order is the assigned multipolarity.

Gamma rays				Conversion electrons									
I	II	III	IV	V	VI	VII	VIII	IX	X	XI	XII		
$E_{\gamma, \text{rel}}$ (keV)	$\Delta E_{\gamma, \text{rel}}$ (keV)	$\Delta I_{\gamma}/100c$	ΔI_{γ} (%)	Remark	Electron shell	E_e (keV)	$I_e/100c$	dI_e/I_e (%)	Measured conversion coefficient I_e/I_{γ}	Theoretical conversion coefficient of Sliv and Band	Multipole order		
										$E1$ $E2$ $M1$			
38.713	0.002	0.17	10	✓	L_2	29.09	11.5	15	68	0.154	70.8	0.563	$E2$
					L_3	30.05	14.2	15	84	0.213	85.7	0.0863	
					M	36.40	3.2	15	19				
41.768	0.010	0.030	...		L_{12}	53.84	0.3	40	3.2	0.117	6.29	1.47	$M1+E2$
47.671	0.010	0.020	...	✓	L_{12}	55.98	0.32	40	0.97	0.108	5.39	1.33	$M1$
54.701	0.004	0.073	10		L_2	57.45	0.20	80	0.61	0.035	5.65	0.016	
63.958	0.003	0.095	20	✓	L_{12}	58.53	0.20	40	0.12	0.0976	4.52	1.19	$E1$
66.097	0.003	0.33	10	✓	L_{12}	59.87	0.29	40	2.4	0.0929	4.13	1.12	$E2+M1$
68.649	0.003	1.65	10	✓	L_3	61.34	0.24	40	2.0	0.0292	4.25	0.0136	
69.990	0.003	0.12	25	✓									
70.488	0.020	0.025	...	✓	L_{12}	65.71	0.83	20	1.14	0.0757	2.85	0.886	$E2+M1$
75.830	0.003	0.73	10	✓	L_3	67.17	0.73	20	1.0	0.0224	2.85	0.0106	
					M	73.52	0.34	30	0.47				
77.912	0.012	0.025	...										
80.885	0.013	0.05	30										
84.253	0.003	0.17	10	Yb^{170}									
85.251	0.015	0.04	30										
87.536	0.016	0.91	20	✓	K	28.15	4.03	20	4.43	0.391	1.31	3.83	$M1$
					L_{12}	77.42	0.39	40	0.36	0.0519	1.51	0.584	
88.942	0.016	0.04	40	✓									
89.866	0.016	0.05	40	✓									
90.224	0.011	0.03	...	✓									
92.653	0.003	0.085	25										
94.528	0.017	0.02	...										
98.586	0.003	0.065	25										
99.660	0.010	0.050	25	✓	K	45.77	0.77	30	1.4	0.243	0.920	2.26	$E2+M1$
105.171	0.005	0.55	10										
107.956	0.004	0.080	15										
109.754	0.015	0.030	15										
111.012	0.004	0.27	10	Tm^{171}									
111.615	0.004	0.050	15										
112.504	0.005	0.040	20		K	55.14	2.02	20	0.62	0.194	0.746	1.77	$E2$
114.544	0.004	3.25	10	✓	L_{12}	104.42	1.11	30	0.34	0.0257	0.476	0.270	
					L_3	105.88	1.23	30	0.40	0.00562	0.370	0.00314	
					M	112.23	0.63	30	0.19				

TABLE IV (continued)

I	II	Gamma rays			V	VI	VII	VIII	IX	Conversion electrons			XII
		III	IV	V						X	XI		
$E_{\gamma,rel}$ (keV)	$\Delta E_{\gamma,rel}$ (keV)	$\Delta I_{\gamma}/100c$	ΔI_{γ} (%)	Remark	Electron shell	E_c (keV)	$I_c/100c$	dI_c/I_c (%)	Measured conversion coefficient I_c/I_{γ}	Theoretical conversion coefficient of Sliv and Band E1 E2 M1	Multipole order		
638.9	0.3	1.1	...										
640.2	0.3	1.0	...										
650.0	0.2	1.5	15										
658.8	0.2	1.7	15										
663.4	0.5	0.60	35										
667.2	0.5	0.50	40										
669.5	0.6	0.50	...										
679.8	0.6	0.60	35										
692.4	0.6	0.30	...	Compl.									
704.2	0.6	1.2	20										
707.3	0.7	0.4	...										
710.0	0.7	0.9	25										
720.4	0.7	1.3	20	✓									
724.1	0.7	0.8	30										
814.1	1.3	0.5	20										
819.9	1.4	0.4	25										
851.5	0.2	0.8	...										
867.9	0.9	0.4	...										

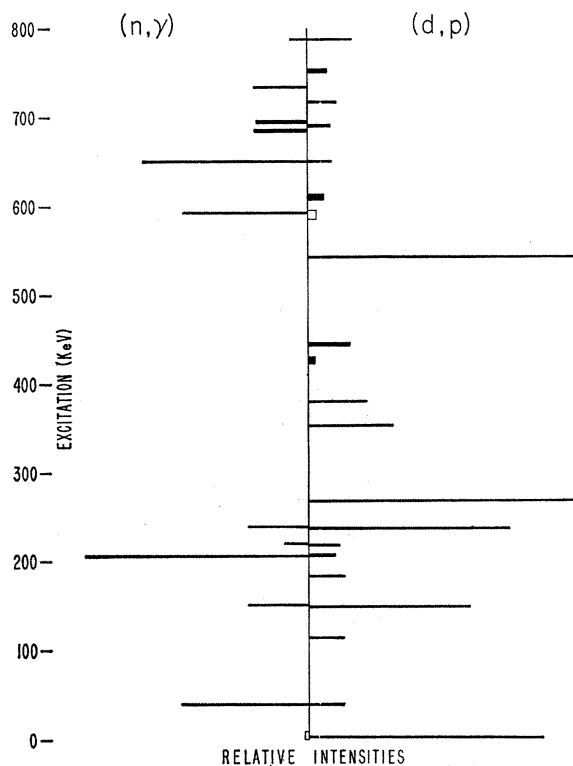


Fig. 5. Histogram showing the comparison of the energies and intensities of the (d,p) and (n,γ) spectra.

calculated with respect to the intensity of the 84.2-keV line of Yb¹⁷⁰ which is emitted during the beta decay of Tm¹⁷⁰. Four lines were found which result from the decay of Tm¹⁷¹ produced by double neutron capture in Tm¹⁶⁹. They are: 111.6, 124.0, 210.6, and 308.5 keV.

The energies and intensities of 52 electron conversion lines have been observed for 29 transitions between 38 and 800 keV. A representative part of the conversion electron spectrum is shown in Fig. 6. Electron intensities at energies <100 keV and the corresponding conversion coefficients are not very reliable owing to the absorption in the detector window. Columns VIII, X, and XII of Table IV list the intensities of all observed electron lines, the conversion coefficients, and the multiplicities which can be assigned. The conversion coefficients were computed from the gamma intensities and the intensities of the conversion electrons. The multiplicities were determined by comparing the conversion coefficients for the various shells with the tables given by Sliv and Band.²¹ Figure 7 shows on a double log-scale the gamma-ray intensities versus the gamma energies. Each gamma transition is represented by a point. Those points shown as triangular were also observed in the conversion-electron spectrum. The full lines mark the

²¹ L. A. Sliv and I. M. Band, *Alpha Beta, and Gamma-Ray Spectroscopy*, edited by Kai Siegbahn (North-Holland Publishing Company, New York, 1965), Appendix 5, Vol. 2.

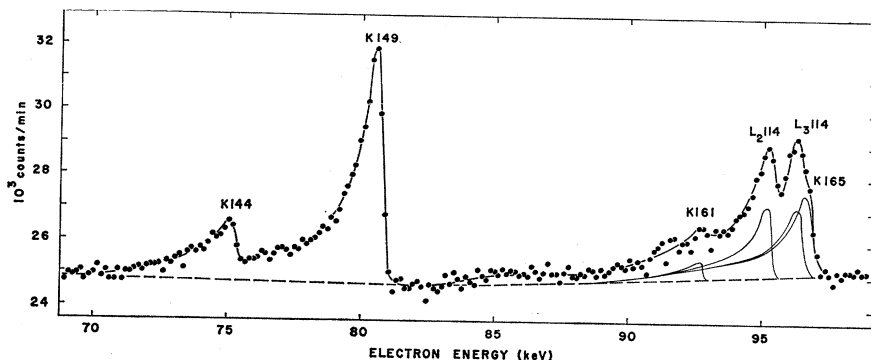


FIG. 6. A representative portion of the low-energy conversion electron spectrum from the reaction $Tm^{169}(n, e^-)Tm^{170}$.

limits for the detection efficiency for K electrons. They are the result of the absorption in the counter window, the thickness of the target, the counting rate of the background, and the magnitude of the conversion coefficients. Therefore different curves are obtained for the various multiplicities. The dashed lines give the limits for the detection of L electrons.

Using 60 transitions from Table IV a level scheme consistent with all the energies and with the multiplicities has been constructed. It comprises 23 states up to an energy of 720 keV. The detailed discussion of the assignment of energy position, spin and parity will be deferred to Sec. III where each state will be discussed in turn and the appropriate Nilsson configurations or vibrational character will be discussed.

III. DISCUSSION

The initial understanding of the Tm^{170} levels, which resulted from the observation of the lowest energy lines

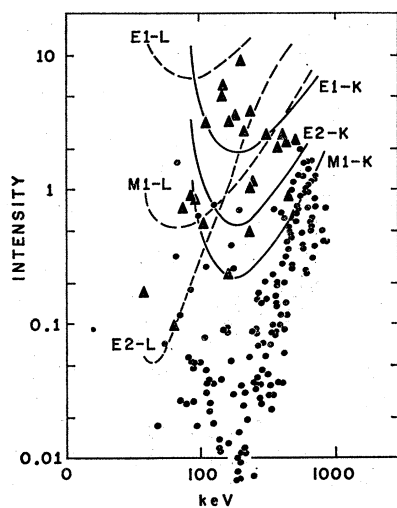


FIG. 7. Intensity versus energy plot for all observed gammas in the low-energy high-resolution spectrum from the reaction $Tm^{169}(n, \gamma)Tm^{170}$. Solid lines represent the limits of detection efficiencies for K electrons for the indicated multiplicities. The dashed lines serve the same purpose for L electrons. Triangular points show that the internal conversion line has been observed.

in the (d, p) reaction and the interpretation of both the energies and cross sections in terms of a single predominant configuration leading to $K=1-$ and $K=0-$ rotational bands, will be presented first. The discussion of all the low-lying intrinsic states and their superimposed rotational bands will then be undertaken in order of increasing energy of excitation. Finally the somewhat higher energy levels which are much less definitely determined and may in part be vibrational in nature will be presented.

A. The (d, p) Cross Sections and the Assignment of the $K=1-$ and $K=0-$ Rotational Bands

In odd- A nuclei, it has been demonstrated that the members of a rotational band built on a particular Nilsson state which are populated in (d, p) stripping show a very characteristic intensity pattern or signature. This property has proven very useful in identifying states in deformed odd- A nuclei. The same technique has been applied with considerable success²²⁻²⁴ to the odd-odd nuclei Ho^{166} and Ta^{182} in spite of the fact that the situation is much more complicated when the odd-odd system is considered as a superposition of two odd- A nuclei. This complication is due to the inclusion of various geometrical factors in the expression for the differential cross section and the fact that more than one value of l_n can contribute to the population of a state. Moreover Coriolis coupling and configuration mixing tend further to complicate the problem. This technique has now been applied to the experimentally determined relative cross sections for the reaction $Tm^{169}(d, p)Tm^{170}$.

By examining the low-lying level structure for odd- A nuclei isotopic and isotonic with Tm^{170} , it is concluded that the important neutron orbitals have the asymptotic quantum numbers $\frac{1}{2}-[521\downarrow]$, $\frac{7}{2}+[633\uparrow]$, $\frac{5}{2}-[512\uparrow]$ and $\frac{7}{2}-[514\downarrow]$, and the proton orbitals are characterized by $\frac{1}{2}+[411\downarrow]$, $\frac{7}{2}+[404\downarrow]$ and $\frac{7}{2}-[523\uparrow]$. Then using Gallagher and Moskowsky's rule, one would expect

²² J. R. Erskine and W. W. Buechner, Phys. Rev. **133**, B370 (1964).

²³ G. L. Struble, J. Kern, and R. K. Sheline, Phys. Rev. **137**, B772 (1965).

²⁴ H. Motz *et al.* (to be published).

TABLE V. Results of the theoretical calculations for the energies and cross sections of the proton groups from the reaction $Tm^{169}(d,p)Tm^{170}$ at a laboratory angle of 45° . Constants used were $B = -43$ keV; $\hbar^2/2\mathcal{I} = 10.0$ keV;

$$\langle K=0^- | H_{int} | K=0^- \rangle - \langle K=1^- | H_{int} | K=1^- \rangle = 187.75 \text{ keV.}$$

State $I\pi$	Calculated energy (keV)	Calculated (d,p) cross section (arbitrary units)	Vector	
			$K=1$	$K=0$
0-	142	0.157	0.0	1.0
1-	233	0.206	0.0012	-0.9999
1-	0	0.191	0.9999	0.0012
2-	212	0.058	-0.2373	-0.9714
2-	30	0.036	-0.9714	0.2373
3-	333	0.105	0.0030	-0.9999
3-	100	0.053	0.9999	0.0030
4-	372	0.090	-0.3705	-0.9288
4-	149	0.012	-0.9288	0.3705

the $p_{\frac{1}{2}}^+ [411\downarrow]$; $n_{\frac{1}{2}}^- [521\downarrow]$: $K=1^-$ state to be the ground state and another low-lying intrinsic state, formed by recoupling the above configuration, to be characterized by $I\pi$, $K=0^-$, 0. Members of bands built on these states can be coupled by the RPC (rotation-particle coupling) term in the rotational Hamiltonian. In order to account for this band mixing, the energy matrix is formed in the basis consisting of the unperturbed states from these bands, and then diagonalized. The resulting wave functions are then used to compute the spectroscopic factors for the (d,p) reaction and a theoretical spectrum is constructed with the aid of DWBA calculations²⁵ for single-particle cross sections. The effects of the neutron-proton residual interaction and the moment of inertia are parametrized. Because there is a $K=0$ band, three parameters are needed: the moment of inertia, the splitting between the $K=1$ and $K=0$ bands due to the $n-p$ force, and the splitting between even and odd members of the $K=0$ band due to the $n-p$ force.

Comparing theory and experiment, an attempt is made to deduce the spins of the levels. Fortunately all nondiagonal matrix elements from the rotational term in the Hamiltonian can be expressed in terms of the proton and the neutron decoupling parameters. Therefore the experimental values ($a_p = -0.87$ and $a_n = 0.85$) have been used. The off-diagonal element contains the factor $[a_p + a_n(-1)^{I+1}]$, where I is the nuclear angular momentum. For states of even spin, the matrix elements become quite large but for odd spin states there is almost no mixing of K values. Because of the energy displacement between even and odd members of the $K=0$ rotational band and the peculiar odd-even band mixing effect, the rotational structure is greatly distorted.

The results of the best fit to the data are given in Fig. 8 and Table V. Empirically it is observed that nondiagonal Coriolis matrix elements are systematically

²⁵ R. H. Bassel, R. M. Drisko, and G. R. Satchler, U. S. Atomic Energy Commission Report ORNL-3240 (unpublished).

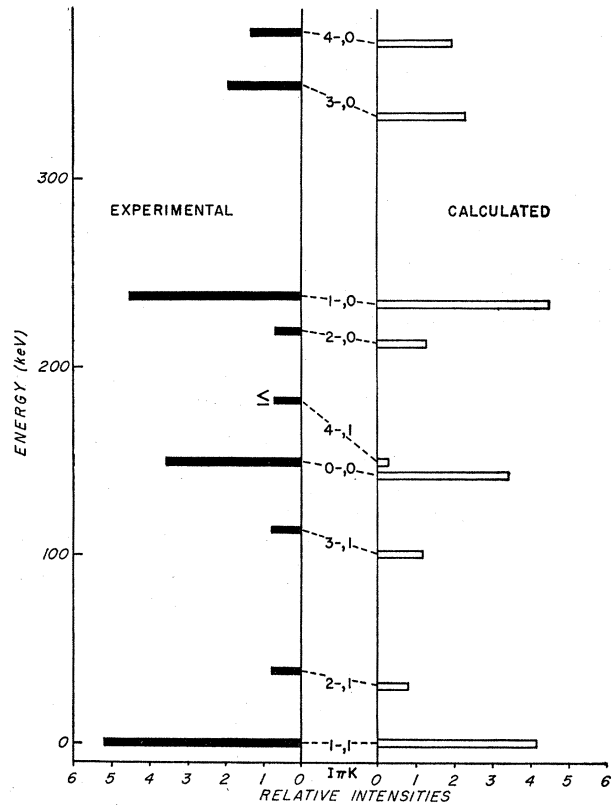


Fig. 8. Experimental (solid bars) and calculated (hollow bars) energies and relative intensities of the proton groups resulting from the reaction $Tm^{169}(d,p)Tm^{170}$ for $K=1^-$ and $K=0^-$ bands.

too large. In this case much better fits are obtained when the matrix elements are reduced by a factor of 2. However their original value was retained in order not to introduce another parameter, since the fit is sufficiently good to validate our spin and parity deductions. This factor of 2 cannot be explained by occupation probabilities predicted by the superfluid model. (The neutron and proton are either diagonal or scattered into their time conjugate states.) However the reduction may be attributed to neglect of mixing that results from the neutron-proton force and the neglect of other configurations in the calculation. Thus, for example, neglect of mixing of the state $p_{\frac{1}{2}}^+ [411\downarrow]$; $m_{\frac{1}{2}}^- [512\uparrow]$: $K=2^-$, might be compensated in part by renormalization of parameters.

B. The Spins, Parities, and Configurations of the Lowest Lying Levels in Tm^{170}

The lowest lying levels of Tm^{170} (up to ~ 450 keV) fit systematically into five intrinsic states and their associate rotational bands resulting from three configurations. In general these states are well established. Usually they are observed in two or all three of the possible experimental methods [(n,γ) and (n,e^-) are here considered equivalent]. These levels are discussed

successively in terms of increasing energies of the levels. The spectroscopic notation used to designate the levels is $I\pi, K$, where I is the total angular momentum, π is the parity, and K is the K quantum number.

1. The $1-, 1$ Ground State

As indicated in the introduction, the ground state of Tm^{170} has a measured spin parity of $1-$. This can be interpreted as the $K=1-$ band head of the configuration $p_{\frac{1}{2}}+[411\downarrow]; n_{\frac{1}{2}}-[521\downarrow]$. The relative intensity of the proton group in the reaction $\text{Tm}^{169}(d,p)\text{Tm}^{170}$ leading to the ground state (see Fig. 8) is strong evidence for both the spin-parity and the configurational assignment. It is, however, particularly interesting that the population of this state with the expected 6595-keV $E1$ gamma transition occurs only very weakly. In view of the fact that the $2-$ member of this band is populated ~ 30 times more and the $1-, 0$ state at 237.246 keV, ~ 15 times more, an unusual forbiddenness of the 6595-keV transition to the $1-, 1$ ground state must be invoked. The reason for this forbiddenness is not evident.

2. The $2-, 1$ 38.713-keV State

A level at 38.713 keV may be inferred from both its population in the (d,p) and high-energy (n,γ) reactions. The accurate determination of the energy of this state results from the observation of a 38.713-keV transition. The conversion electron data of Table IV suggest a total conversion coefficient α of ~ 170 . Experimental difficulties in determining α at low energies mentioned in Sec. II D make this determination inaccurate. The total conversion coefficient predicted²¹ for a pure $E2$ transition is ~ 200 whereas that for a pure $M1$ is less by more than an order of magnitude. Thus, the experimental α_{total} suggests that $E2/M1 > 1$. The spin-parity and configurational assignment are evident both from the $E2/M1$ ratio and from the relative population of the level in the (d,p) reaction. The $2-$ state, at 38.713 keV, then, is the first rotational member on the $K=1-$ ground state.

3. The $3-, 1$ 114.543-keV State

The third member of this rotational band is observed at 114.543 keV. This $3-$ state can be inferred both from the 114.543 ± 0.002 -keV pure $E2$ ground-state transition and from the sum $38.713 \text{ keV} + 75.830 \text{ keV} = 114.543 \pm 0.03 \text{ keV}$. The cross-section in the reaction $\text{Tm}^{169}(d,p)\text{Tm}^{170}$ for populating the 114.543-keV state is consistent with the assignment.

The mixing ratio $T(E2)/T(M1)$ for the 75.83-keV transition is measured to be 0.9. Using this value it should be possible to calculate this mixing ratio in the 38.721-keV transition using the following expression:

$$\frac{T_{38.7}(E2)}{T_{38.7}(M1)} = \left(\frac{38.7}{75.8}\right)^2 \frac{\langle 2210 | 2211 \rangle^2 \langle 3110 | 3121 \rangle^2}{\langle 2110 | 2111 \rangle^2 \langle 3210 | 3221 \rangle^2} \times 0.9.$$

This calculation gives 1.9 for the ratio which agrees within the experimental error with the measured value (Sec. III B 2).

4. The $0-, 0$ State at 149.721 keV

All three experimental methods indicate the existence of a level at 149.721 keV. The high (d,p) cross section is in excellent agreement with the $0-, 0$ assignment. Furthermore, there is an intense relatively pure 149.718-keV $M1$ transition to the ground state and a considerably weaker 111.012-keV transition which combines with the 38.713-keV transition to give the sum $149.725 \pm 0.005 \text{ keV}$. We may, therefore, be reasonably certain of the $0-, 0$ assignment. The $K=0-$ band results from the alternative coupling of the same $[411\uparrow]$ proton and $[521\downarrow]$ neutron orbitals used in constructing the $K=1-$ band. Details of the approximate cancellation of the Coriolis coupling between the odd-spin members of the $K=0-$ and $K=1-$ bands are given in Sec. III A and in Sec. IV.

5. The $4-, 1$ State at 183.57 keV

This state is clearly observed in the (d,p) reaction at an excitation energy of $183.3 \pm 1.1 \text{ keV}$. The cross section for its population is consistent with its interpretation (see Fig. 8) as the $4-$ rotational member of the $K=1-$ rotational band. The calculated cross section of the (d,p) reaction to the $3+, 3$ state at 183.193 keV, almost coincident in energy with the $4-, 1$ state at 183.3 keV, is expected to be an order of magnitude less than the observed cross section. Thus the main contribution to the proton group observed at 183 keV must be from the $4-, 1$ state. For this reason, however, the experimental cross-section shown for the $4-, 1$ state in Fig. 8 is shown as an upper limit.

The $4-, 1$ state should not be directly populated by high-energy neutron-capture gamma rays but might be weakly populated by low-energy gamma rays cascading through intermediate states. Population considerations suggest a feeding of this state of the order of $0.5/100n$. The depopulation of the 183.3 ± 1.1 -keV state whose energy is defined by the (d,p) reaction would then predict gamma rays of 144.6 ± 1.1 and $68.8 \pm 1.1 \text{ keV}$ to the $2-$ and $3-$ members of $K=1-$ band.

We have searched very carefully for these lines. Unfortunately the (d,p) energy does not define them very exactly. Furthermore they are expected in the vicinity of the strong lines at 144.482 and 68.649 keV. The respective parts of the spectrum have been measured in second-order reflection to achieve optimum sensitivity and in fifth-order reflection to achieve maximum resolution. The results are shown in Figs. 9 and 10. The data from second-order reflection (Fig. 9) show two predominant peaks at 144.48 and 149.72 keV and a weak line at 144.86 keV. The apparent indication of a peak at 146.4 keV is due to a strong third-order reflection of the 219.68-keV transition, and the nonvanishing

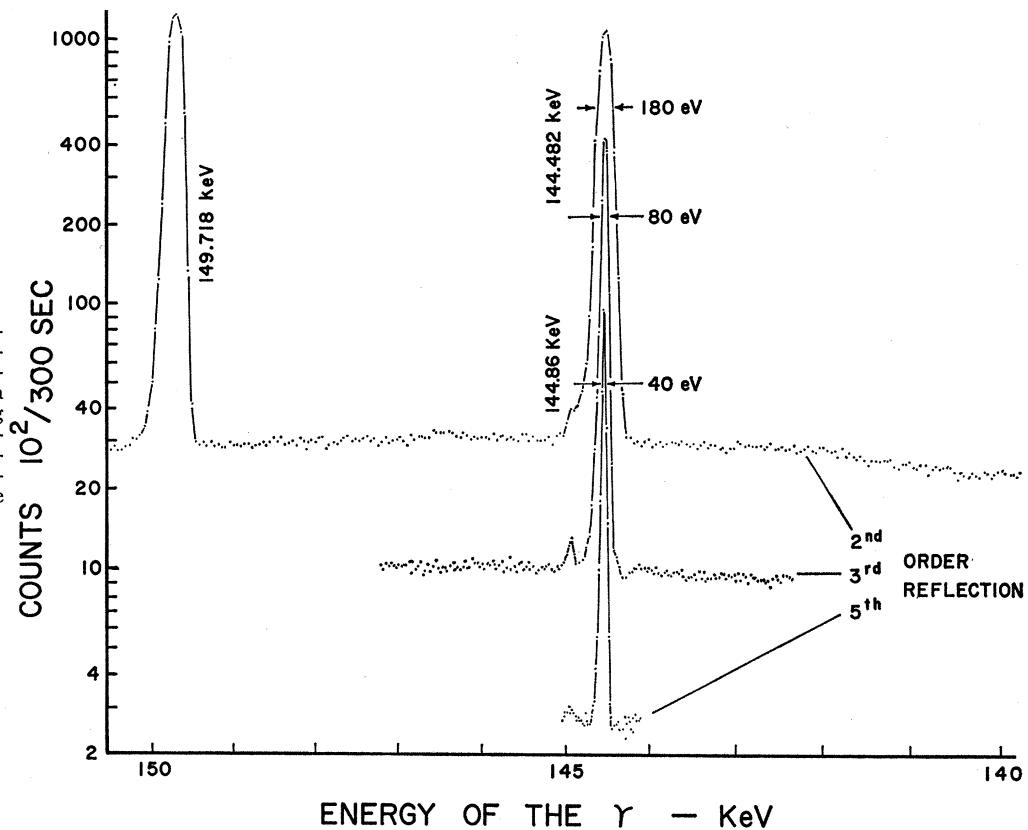


FIG. 9. The 140–150-keV portion of the low-energy gamma spectrum from the reaction $Tm^{169}(n,\gamma)Tm^{170}$ using the Risø curved crystal spectrometer. Second-, third-, and fifth-order reflections are shown.

probability of the NaI detector to produce pulses, the height of which just falls into the channel which has been set to accept the full energy line of 140–150-keV radiation. The 144.4- and 144.8-keV lines are clearly separated in the third order of reflection. The fifth order of reflection shows that there is no additional prominent line in the immediate neighborhood of the 144.48-keV peak since the full width at half-maximum is only 40 eV.

The gamma transitions in the 68-keV region are shown in Fig. 10. The peak at 70.11 keV is due to the strong 105.17-keV transition which appears as a third-order reflection. The insert shows the fifth-order reflection of the 68.64-keV line which clearly appears as a single line even under the high resolution attainable at the Risø curved-crystal spectrometer. During the measurement of the data shown in Fig. 10, the source was turned through a small angle around its vertical axis in order to gain intensity by decreasing the effective source depth and thus the gamma-ray absorption within the source. This absorption is observable if a source is aligned for maximum resolution. For this reason the full width at half-maximum of the fifth order of reflection of the 68-keV line is 15 eV instead of 9 eV.

As a result of this careful search there would appear to be two possibilities:

(a) The $4-, 1$ state may be so close in energy to the $3+, 3$ state at 183.193 keV that the depopulating lines

are masked by the strong lines depopulating the 183.193-keV state. This would require the $4-, 1$ state to lie within 100 eV of the state at 183.193 keV and is therefore somewhat improbable.

(b) The $4-, 1$ state may be defined by the 144.86-keV line to lie at 183.57 keV. The other expected line at 69.03 keV may be weaker than the limit of observation (i.e., $<0.003/100n$). If we assume that the mixing of the $K=1$ and the $K=0$ bands does not strongly affect the branching ratios of the intraband $E2$ and mixed $E2+M1$ transitions, we calculate the 69.03-keV $E2$ gamma intensity to be $\sim 0.0003/100n$. Making the same assumption and using the measured branching ratio from the 114.543-keV state, the rotational model yields a 69.03-keV $M1$ gamma intensity of $\sim 0.0008/100n$. Thus the total intensity expected for the 69.03-keV gamma is $\sim 0.001/100n$ which is well below our observable limit of $0.003/100n$.

Accordingly we favor the second alternative and tentatively assign an energy for the $4-, 1$ state of 183.57 keV. However in view of the fact that only a single transition is observed depopulating this state, the transition is shown dashed in Fig. 11. Furthermore the energy uncertainty (1.1 keV) of the (d,p) measurement is retained and the level is shown broad.

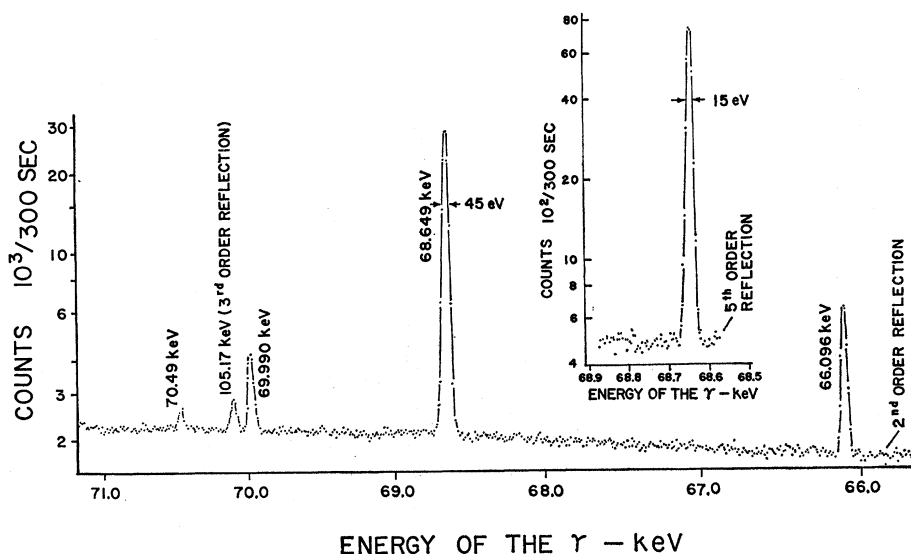


Fig. 10. The 66–71-keV portion of the low-energy gamma spectrum in second-order reflection from the reaction $\text{Tm}^{169}(n,\gamma)\text{Tm}^{170}$ using the Risø curved crystal spectrometer. The insert shows the spectrum in the vicinity of the 68.649-keV line in the fifth-order reflection.

6. The $3+, 3$ State at 183.193 keV

This state is not observed in either the (d,p) or high-energy (n,γ) reactions. The possible (d,p) population of this state would be masked by the considerably larger population of the $4-, 1$ state with which this state is approximately degenerate in energy. The high-energy (n,γ) transition to this state would be $M2$, and is not expected to be observed. Two $E1$ transitions have been observed with energies of 68.649 ± 0.003 and 144.482 ± 0.004 keV. These transitions depopulate the state at 183.193 keV leading to the $3-, 1$ and $2-, 1$ states, respectively, and imply a spin $3+$ for this state. We believe the correct Nilsson assignment is $p_{\frac{1}{2}}^+ + [411\downarrow]$; $n_{\frac{7}{2}}^+ + [633\uparrow]$: $3+$. This corresponds to promoting a neutron in the $\frac{7}{2}+$ orbital into the $\frac{1}{2}-$ orbital, thus creating a hole state. Of the six fairly definitely known $\frac{7}{2}^+ + [633\uparrow] - \frac{1}{2} - [521\downarrow]$ energy differences for 99, 101, and 103 odd-neutron species,^{26,27} this energy difference varies from 24 keV in Yb^{169} to 207 keV in Er^{167} . Therefore, the 183-keV energy difference observed in Tm^{170} is reasonable. The $3+, 3$ assignment to the 183.193-keV state suggests that the 68.649- and 144.482-keV $E1$ transitions are K forbidden. A search for $M2$ or $E3$ mixing in the 144.482-keV transitions indicates that it is $< 1\%$. Nonetheless, the lifetime of the 183.193-keV state should be measured and should give evidence of the K forbiddenness of the transitions depopulating it.²⁸

²⁶ B. R. Mottelson and S. G. Nilsson, Kgl. Danske Videnskab. Selskab, Mat. Fys. Skrifter I, No. 8 (1959).

²⁷ R. K. Shelin, W. N. Shelton, H. T. Motz, and R. E. Carter, Phys. Rev. **136**, B351 (1964).

²⁸ Since this paper was completed, R. Kastner, A. Andreeff, and P. Manfrass [Paper 50, Antwerp Meeting, 1965 (unpublished)] have measured the half-life of the 183.193-keV state to be $4.2 \mu\text{sec}$.

7. The $2-, 2$ State at 204.452 keV

This state is observed by all three methods. The use of the low-energy (n,γ) and (n,e^-) spectra and the Ritz combination principle is decisive in its assignment, because the (d,p) line is not completely resolved from the level at 219.713 keV. The 204.451-keV line is the most intense low-energy gamma radiation observed, which suggests a band head depopulation. It is clearly a ground-state transition, since it represents the crossover for the combination 38.713 and 165.741 keV. The measured multipolarity for the 165.741 and 204.451 keV transitions are $M1$ and $M1 + E2$, respectively. The mixing for the 204.451-keV line is $(40 \pm 20)\%$ $E2$ and $(60 \pm 20)\%$ $M1$. These data suggest the assignment $I\pi, K=2-, 2$. A $K=0$ assignment would give a branching ratio from the 204.452-keV state such that the intensity of the 165.741-keV transition would be 18 ± 6 . The experimentally measured value is 3.3 ± 0.3 in fair agreement with the predicted intensity (5.9 ± 1.7) assuming $K=2$. If an admixture of $K=0$ in the $2-$ state and the lack of it in the $1-$ ground-state band is considered (Table V), the agreement is even better. We believe the $I\pi, K=2-, 2$ assignment results from the promotion of the neutron from $\frac{1}{2}- [521\downarrow]$ orbital to the $\frac{5}{2}- [512\uparrow]$ orbital. Of the five fairly definite $\frac{5}{2}- [512\uparrow] - \frac{1}{2}- [521\downarrow]$ neutron-energy differences in the 99, 101, and 103 odd- A neutron species,^{26,27} this energy difference varies from 76 keV in Dy^{165} to 392 keV in Yb^{173} . Thus the 204-keV assignment in Tm^{170} is reasonable.

8. The $2-, 0$ 219.713-keV State

This state is clearly observed with all three experimental methods. The (d,p) cross section to this state is consistent with its interpretation as the $2-$ state built on the $K=0-$ band head at 149.721 keV (see Fig. 8). Furthermore, the depopulation of the state gives strong

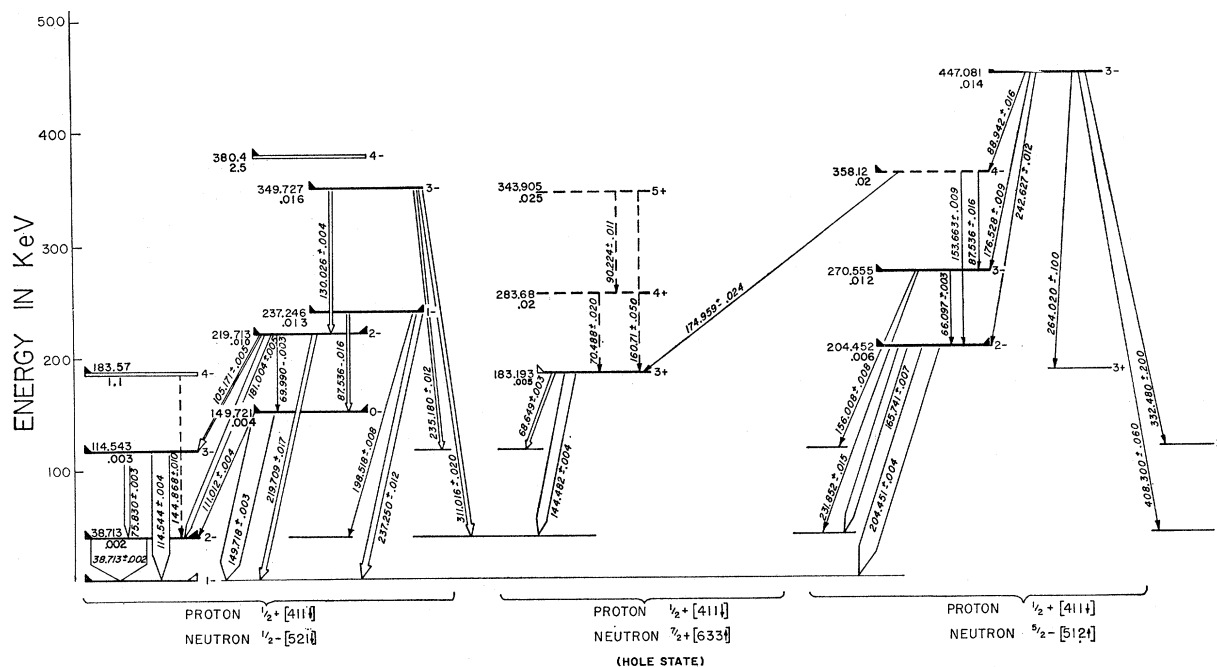


FIG. 11. Lowest lying energy levels in Tm^{170} . For the complete level scheme Figs. 11 and 12 should be combined. See the text (III B 16) for detailed descriptions of symbols, etc.

evidence for the assignment. The 69.990-keV transition to the band head is not able to compete as well as might be expected with the higher energy transitions to the ground-state band because of the mixing of this $K=0-$ band into the ground-state band. The mixture in the 219.708 ± 0.017 -keV line is judged from the K conversion coefficient to be $\sim 30\%$ $M1$ and $\sim 70\%$ $E2$. This is not inconsistent with the amount of $M1$ expected when it is recognized that there is considerable $K=1-$ admixture in the state at 219.713 keV. This assignment also explains the mixing of $50 \pm 10\%$ $E2$ and $50 \pm 10\%$ $M1$ observed for the 181.004-keV transition which cascades through the 38.713 keV $2-$, 1 state.

9. The $1-, 0$ 237.246-keV State

This state is observed in all three experiments. The high (d,p) cross section (see Fig. 8) suggests the assignment $1-, 0$. The existence of this state is also indicated in the energy agreement between the three sets of transitions which depopulate this state. Furthermore both the facts that this state belongs to the $K=0-$ band and that the $K=1-$ band is mixed with the $K=0-$ band are revealed in the way this state is depopulated. The energy of the state is clear evidence of another case in which the even and odd members of a $K=0$ band are split.

10. The $4+, 3$ and $5+, 3$ States at 283.68 and 343.905 keV

Evidence for these states comes solely from the low-energy (n,γ) spectrum. The existence of a band in-

volving $3+$, $4+$, and $5+$ states with the moment of inertia of this band taken to be close to that in Ho^{166} provides a basis for the tentative assignment of these states. Neither the high-energy (n,γ) nor the (d,p) reaction is expected to populate these states appreciably. Furthermore, K selection rules keep the $4+$ and $5+$ members of the band from depopulating appreciably to other bands. Thus, although all the evidence for the band has been found which can reasonably be expected utilizing the three methods, the evidence is not very strong. It rests on the three weak gamma rays— 70.488 ± 0.020 , 90.224 ± 0.011 , and 160.71 ± 0.05 keV and the fact that the sum of the energies of the first two agrees with the energy of the third. It should be pointed out also that the energies do not fit the expected $I(I+1)$ energy sequence very well. If the form $E = (\hbar^2/2\mathcal{I})I(I+1) - BI^2(I+1)^2$ is assumed the B coefficient is defined by the energy levels to be -11.7 eV which is larger than usual. For these reasons the levels are shown dashed in the level scheme.

11. The $3-, 2$ State at 270.555 keV

This state is observed in both low-energy (n,γ) and rather strongly in the (d,p) experiments. Depopulation occurs both to the $K=1-$ ground state and within the band. The strong excitation of this state and its depopulation are all consistent with its assignment as the first rotational member built on the $2-, 2$ band at 204.452 keV.

12. The $3-, 0$ State at 349.727 keV

This state is populated in the (d,p) reaction, and depopulation is seen in the low-energy (n,γ) spectrum. Furthermore both the calculated (d,p) cross section and the calculated energy for this state are more nearly in agreement with its assignment as $3-, 0$ than with the other possible assignment of $4-, 0$ (see Fig. 8). Three transitions from the low-energy (n,γ) spectra accurately define the energy of the state and also suggest the $3-, 0$ assignment. The intraband transition to the $2-, 0$ state is strong as expected for an odd to even spin transition. The transition to $2-, 1$ and $3-, 1$ states are relatively strong whereas there is no evidence of a transition to the $1-, 1$ ground state. This is evidence for the relatively large transition probability of the $M1$ transitions (see IV. Conclusions).

13. The $4-, 2$ State at 358.12 keV

This state is observed in both the low-energy neutron-capture gamma-ray spectroscopy and in the (d,p) reaction although the (d,p) reaction suggests an excitation energy of 353.2 keV which is considerably poorer agreement than that usually obtained. Three transitions appear to depopulate the state and thereby help to define its energy. Two of the transitions are intraband transitions and the other is a transition to the $3+, 3$ band head. Since this latter transition is expected to be $E1$, although the multipolarity of this relatively weak transition has not been measured, all is consistent with the $4-, 2$ assignment.

14. The $4-, 0$ State at 380.4 keV

This state is observed only in the (d,p) experiment. However, the agreement between the energy and cross section for the population of this state with theory lends support to this assignment.

15. The $3-, 3$ State at 447.079 keV

The existence of this state is demonstrated both by its population in the (d,p) reaction and its depopulation by five gamma rays. The fact that fairly low-energy transitions populate four different $K=2$ and 3 states suggests a relatively high K value. Furthermore the strong population of all observed members of the $K=2-$ band suggests that this is the band head resulting from the recoupling of the Nilsson orbitals from the $K=2-$ band to give the $K=3-$ band.

16. Level Scheme of the Lowest Energy Levels

Figure 11 summarizes the data presented above in Sec. III B. Solid or dashed levels indicate that the energy has been precisely determined with the high-resolution low-energy (n,γ) spectra. A hollow level means that the energy of the level has been obtained in the (d,p) reac-

tion only and is therefore less accurately known. The energy in kilo-electron-volts is listed on the left side of each level with uncertainty written immediately below. A triangle on the left-hand edge of the level signifies (d,p) population and on the right-hand-side high-energy (n,γ) population. Hollow triangles indicate that the evidence for population is not conclusive. All observed transitions between levels are shown. The width of the arrow indicates the total gamma-ray and electron intensity of the transition. Nilsson assignments are shown at the bottom of the figure. It is significant that 16 states fit into five rotational bands resulting from the three configurations in which the proton orbital stays fixed as $\frac{1}{2}+[411\downarrow]$ while the neutron orbital changes from $\frac{1}{2}-[521\downarrow]$ to $\frac{7}{2}+[633\uparrow]$ and then to $\frac{5}{2}-[512\uparrow]$, and that the Gallagher-Moszkowski coupling rules are obeyed.

C. The Higher Energy States in Tm^{170} and the Possible Observation of $K=2$ Gamma Vibrations in an Odd-Odd Nucleus

A number of higher energy states have been observed in Tm^{170} . For the most part these states have not been interpreted. When, however, the high-resolution, low-energy neutron-capture gamma-ray spectra define the energy of a state and to some extent its character, interpretation has been attempted. It should, however, be clearly pointed out that in the seven states to be discussed here briefly, only three have also been observed in (d,p) reaction spectra. Consequently both the character and validity of all of the levels presented here are less certain than any of the levels, with the possible exceptions of the dashed levels presented in Fig. 11.

1. The 411.45-, 456.25- and 512.35-keV States and the Possible Existence of a $K=2$ Gamma Vibrational Band Built on the $K=1-$ Ground-State Band

These three states are calculated from a series of energy loops involving low-energy (n,γ) transitions. None of them is observed in either the (d,p) or the high-energy (n,γ) experiments. These states are not seen in the high-energy (n,γ) in spite of the expected $E1$ nature of the transitions to them similar to the $E1$ ground-state transition. The fact that eight of the nine transitions depopulating these states go to the ground-state band suggests that these three states are related. The approximate rotational nature of their energy spacings is also indicative of this. The close relationship of this new band to the ground-state band also suggests that it might be the $K=2$ gamma vibrational band with $K=1-$ built on the ground-state band. The strong $E2$ transitions from the 411.45-keV state to the ground state is also strongly suggestive of this assignment. In view of the fact that no spins have been uniquely defined, these assignments must be considered tentative.

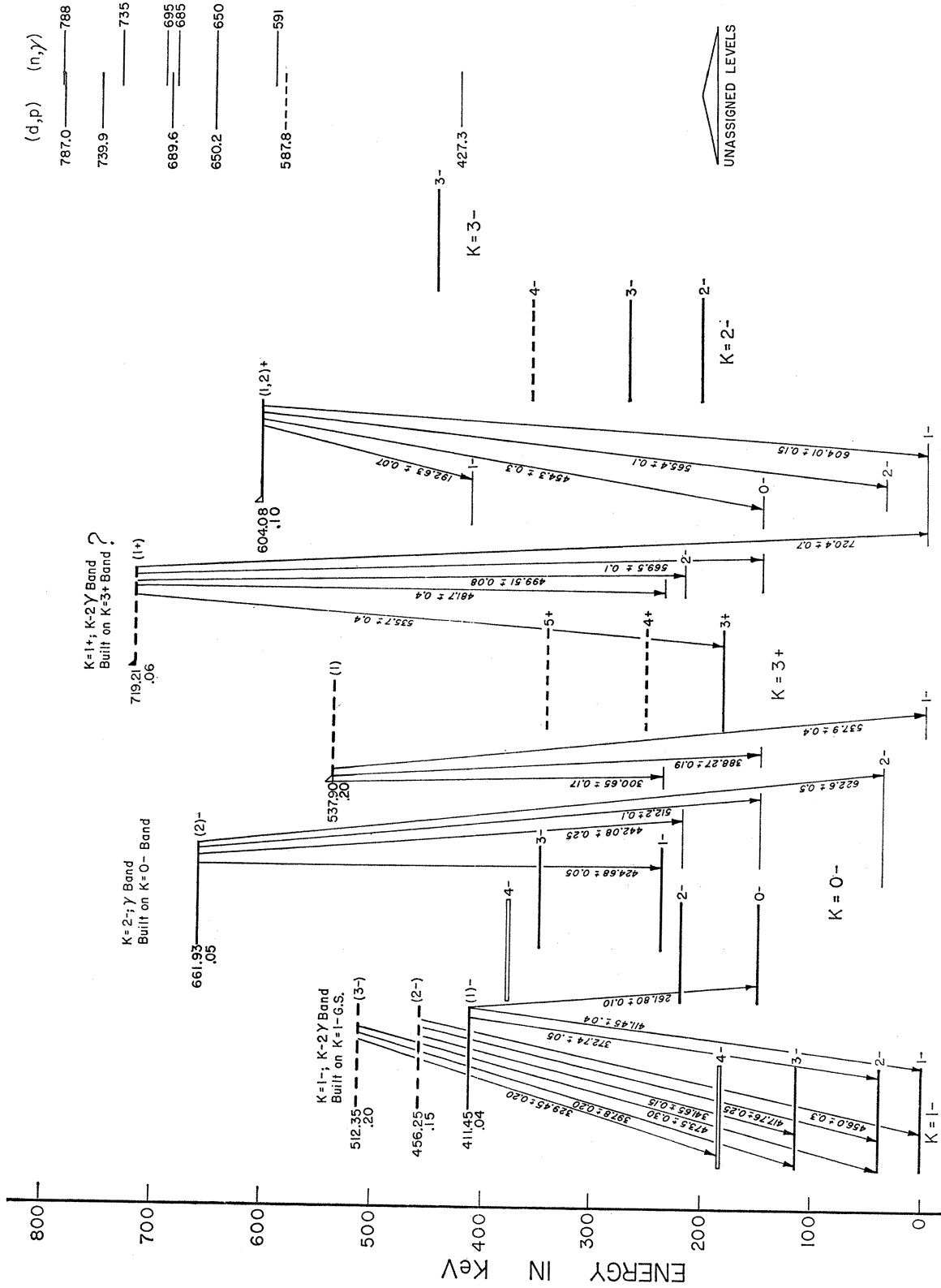


FIG. 12. Higher lying energy levels in Tm^{170} . For the complete level scheme Figs. 11 and 12 should be combined. See the text (III B 16 and III C 6) for detailed descriptions of symbols, etc.

2. *The 661.93-keV State and the Possible Existence of a Gamma Band Built on the $K=0-$ Band with $K=2-$*

Four low-energy transitions define a state at 661.93 keV. This state is not seen in either (d,p) or high-energy neutron-capture gamma spectra. The strong $E2$ depopulation of this state to the $0-, 0$ band head suggests a γ vibrational assignment. The other three transitions depopulating this state are all consistent with this assignment in view of the close relationship they establish with the other members of the $K=0-$ band and the $K=1-$ band.

3. *The 719.21-keV State and the Possible Existence of the $K-2 \gamma$ Band Built on the $K=3+$ Band*

This state is established both by (d,p) population and by five transitions which depopulate it. Since none of these transitions has measured multiplicities, even the parity of the state is in doubt. However its decay is consistent with its assignment as the $K-2$ gamma vibrational band built on the $K=3+$ band. In view of the failure to determine either spin or parity this assignment is considered more questionable than either of the two previous assignments. Consequently it is shown as questionable in Fig. 12.

4. *The 537.90- and 604.08-keV States*

These two states are computed using the Ritz combination principle and the low-energy (n,γ) transitions. They also are tentatively identified in the (d,p) spectra. The 537.90-keV state has three transitions depopulating it which suggest it should have low spin and low K quantum number. In view of the gamma population of the $0-$ state, spin 1 seems the most likely assignment. The 604.08-keV state depopulates via four transitions all of which go to the $K=0-$ and $K=1-$ bands. The measured $E1$ multipolarity then suggests spin 1 or 2 and even parity.

5. *Unassigned States*

Those states which do not fit into the level systematics shown in Figs. 11 and 12 are presented on the right-hand side of Fig. 12. For the most part these are high-energy states.

6. *Summary of the High-Energy States in Fig. 12*

Figure 12 presents the summary of the high-energy states in Tm^{170} and their assignments when possible. The conventions followed are the same as in Fig. 11. The low-energy states of Fig. 11 are included but for clarity only the previously unassigned transitions are presented.

7. *Uncertainties in the High-Energy Transitions*

It is well to emphasize the much greater uncertainty about the assignment and even the existence of these

higher energy states. Figure 12 must be considered highly tentative. The much greater error in energy in these higher energy transitions considerably reduces the power of the Ritz combination principle. Consider, for example, the 604.08-keV state. There is a probability of 53% that a line of energy between 300 and 600 keV with an average error of 200 eV will by chance fit between the 604-keV state and some one of the lower levels. The probability of four such transitions is therefore 7.9%. Thus the possibility for finding such a random set of combinations is not negligible. In those cases where this probability is greater than 10% the levels in Fig. 12 are drawn dashed.

IV. CONCLUSIONS

A. The Nilsson Assignments in Tm^{170}

The three lowest lying Nilsson configurations in which the proton orbital Ω_p is $\frac{1}{2}+[411\downarrow]$ and the neutron orbital, Ω_n , is successively $\frac{1}{2}-[521\downarrow]$, $\frac{7}{2}+[633\uparrow]$ and $\frac{5}{2}-[512\uparrow]$ accounts for 16 states in the low-energy excitation of Tm^{170} . Furthermore, five of the six rotational bands expected from these configurations are observed, and thus give a fairly complete set.

B. Coriolis Coupling in Tm^{170}

The Coriolis coupling between the $K=0-$ and $K=1-$ bands is expected to produce an anomaly in the rotational structure of the $K=1-$ ground-state band.²⁹ Indeed as pointed out in Sec. III A and graphically illustrated in Table V, the anomaly is accentuated by the almost complete cancellation of this coupling in the odd- I states. This results from the general form of the Coriolis coupling term,

$$(-\hbar^2/2\mathfrak{F})[I(I+1)]^{1/2}[a_p+a_n(-1)^{I+1}],$$

and the fact that the decoupling parameters, a_p and a_n , are approximately equal in magnitude and of opposite sign.

Hansen *et al.*⁷ have observed the same $K=1-$ and $K=0-$ rotational bands in Tm^{172} utilizing the decay of Er^{172} . It is particularly interesting to note that the spacing between the $I=2-$ and $I=1-$ members of the $K=1-$ rotational band in Tm^{172} with the same configuration as that in Tm^{170} is 38.7 keV in exact duplication of these results. However, in view of the fact that $K=0-$ band head of the same configuration occurs 68 keV above the $K=1-$ state in Tm^{172} in contrast to 149.7 keV above the $K=1-$ state in Tm^{170} , the close agreement in rotational spectra results from a series of complex coincidences rather than an especially great similarity of the rotational states in Tm^{170} and Tm^{172} .

If the phenomenological rotational form,

$$E = (\hbar^2/2\mathfrak{F})I(I+1) - BI^2(I+1)^2,$$

²⁹ A. K. Kerman, Kgl. Danske Videnskab. Selskab, Mat. Fys. Medd. 30, No. 15 (1956).

is assumed for the $K=2$ γ -vibrational band at 411.45 keV, the value for B obtained is 185 eV. This value is much higher than usual for such rotational bands (see for example the rotational bands in Ho¹⁶⁶). It is entirely possible that this effect is largely due to the combination of the inherited anomalous rotational structure from the ground-state band and the Coriolis coupling with the $K=0$ band. These effects may, however, be overshadowed by Coriolis coupling of other bands not yet investigated in Tm¹⁷⁰.

C. Calculation of the Energies and (d,p) Cross Sections for the $K=1-$, and $K=0-$ Bands

It has generally been conceded that mixing of levels close to the ground state will produce particularly complex low-lying states in odd-odd nuclei. For this reason the calculation of both the energies and the (d,p) cross sections for the various rotational members of the $K=1-$ and $K=0-$ bands is particularly significant. The rather good agreement between experiment and theory was accomplished using only three proton and four neutron orbitals. The Coriolis coupling between the $K=1-$ and $K=0-$ bands was reasonably well reproduced. The much greater mixing of even- I states is obvious both in experiment and calculation.

However, a much more sensitive test of the correctness of the theoretical calculations would be an attempt to reproduce transition probabilities or their ratios. This is beyond the scope of the present investigation but will be attempted in future research.

D. The Possible Experimental Observation of γ -Vibrations in Odd-Odd Nuclei

Three states or bands have been suggested which are assigned as $K=2$ γ -vibrational bands. Since no spins have been definitely measured, these assignments are based entirely on the modes of decay and must be considered highly tentative.

The fact that the lowest lying states in odd-odd nuclei are two quasiparticles suggests that the collective character of gamma vibrational bands might be considerably less in odd-odd nuclei than in neighboring odd- A nuclei. The rather strong $E2$ transitions to the band heads of the parent bands observed in these experiments may suggest that there is still considerable collective nature if these assignments are correct. The energies of the gamma bands above the parent bands; 411, 511, and 536 keV for $K=1-$, $K=0-$, and $K=3+$ bands, respectively, are not unreasonable. It is known that the $K=2$ gamma vibration in Tm¹⁶⁹ lies at 570 keV.³⁰ Since there are two quasiparticles in Tm¹⁷⁰, the gamma vibrations should lie somewhat lower in this nucleus.

³⁰ R. M. Diamond, B. Elbek, and F. S. Stephens, Nucl. Phys. **43**, 560 (1963).

E. High Transition Probability of the $M1$ Transitions in the $K=0$ Rotational Bands in Odd-Odd Nuclei

One of the obvious facts in the $K=0-$ band is the relatively high transition probability for $M1$ in comparison to $E2$ transitions. This results presumably from the especially allowed nature of the $M1$ transitions and seems to be characteristic of $K=0$ rotational bands of odd-odd nuclei.³¹

F. Evidence for a Direct Reaction Mechanism in the High-Energy (n,γ) Process

One of the most striking features of the high-energy Tm¹⁶⁹ (n,γ) Tm¹⁷⁰ process is the fact that this reaction appears to select neutron configurations rather than proton configurations for excitation. The density of excited proton and excited neutron states in the low-energy region in Tm¹⁷⁰ should be approximately equivalent. Yet up to an energy of ~ 750 keV the high-energy (n,γ) reaction excites only states which have been excited in the (d,p) reaction.

The similarities between the high-energy (n,γ) and the (d,p) processes have been thoroughly reviewed by Groshev *et al.*³² Even the intensity ratios for the two processes have been quantitatively considered by Bockelman³³ who found that this ratio is confined within fairly narrow limits for a number of light nuclei. On the other hand, Ikegami and Emery^{34,35} have carefully documented an anticorrelation between the $B(E1)$ values in high-energy (n,γ) and the spectroscopic factor for (d,p) stripping to Fe⁵⁵ and Fe⁵⁷. This fact was interpreted in terms of the capture into "doorway states" of seniority three, leading to intermediate structure in the compound system, whose subsequent decay into states of low excitation by high-energy gamma rays could not populate simple single-seniority states populated by the (d,p) reaction.

It should also be noted that in the case of the (d,p) and (n,γ) reactions leading to Y⁹⁰, the strongest high-energy gamma ray³⁶ populates the $2+$ state resulting from an excited proton configuration, which is populated³⁷ to less than 1 part in 1000 (relative to the ground state) in the (d,p) reaction. Yet neutron configurations are populated by both the high-energy (n,γ) and (d,p) reactions.

The experimental results presented here seem to

³¹ B. R. Mottelson (private communication).

³² L. V. Groshev, A. M. Demidov, V. N. Lutsenko, and V. I. Pelekhov, *Proceedings of the Second International Conference on the Peaceful Uses Atomic Energy, Geneva-1958* (United Nations, Geneva, 1958), Vol. 15, p. 138.

³³ C. K. Bockelman, Nucl. Phys. **13**, 205 (1959).

³⁴ A. Kerman, L. S. Rodberg, and J. E. Young, Phys. Rev. Letters **11**, 422 (1963).

³⁵ H. Ikegami and G. T. Emery, Phys. Rev. Letters **13**, 26 (1964).

³⁶ G. A. Bartholomew, P. J. Champion, J. W. Knowles, and G. Manning, Nucl. Phys. **10**, 590 (1959).

³⁷ C. Watson, C. F. Moore, and R. K. Shelton, Nucl. Phys. **54**, 519 (194).

indicate that the high-energy (n,γ) reaction on Tm^{169} is a direct reaction which utilizes a relatively small part of the total slow-neutron cross section and tends to populate neutron states somewhat exclusively. The observation of a similar effect in the $\text{Ho}^{166}(n,\gamma)\text{Ho}^{166}$ reaction is corroborative evidence for this suggestion in a nucleus which differs from Tm^{170} by only four mass units.

The fact that there is sometimes correlation and sometimes anticorrelation between (n,γ) and (d,p) reactions is probably to be understood in terms of the specific character of the capturing states. The surprising weakness of the expected $E1$ transition to the ground state of Tm^{170} is perhaps additional evidence for this individuality.

G. Experimental Techniques for Complex Nuclei

This experiment demonstrates again the importance of the application of a variety of the best techniques in solving some of the complex spectroscopic problems presented by odd-odd nuclei. The application of (d,p) reaction spectroscopy, high-energy neutron capture γ -ray spectroscopy, and low-energy neutron capture γ -ray and electron spectroscopy are successful complementary methods. Furthermore, it seems probable that still

additional methods, such as ($d,p\gamma$) and ($n,\gamma\gamma$), must be brought to bear if considerable additional progress is to be achieved. It should be pointed out that, although in Tm^{170} we have progressed in this publication from knowledge of only the ground state to knowledge of some 23 states, this is only a beginning. For example, we have studied only the first 720 keV of excitation, and we have not observed excited proton configurations or any four quasiparticle states.

ACKNOWLEDGMENTS

We wish to thank Professor H. Maier-Leibnitz and Professor O. Kofoed-Hansen for their interest in, and sponsorship of, part of this research. Discussions held with B. R. Mottleson, Arthur Kerman, Peter Axel, and James Griffin were particularly helpful. We wish to thank the staff of the Tandem Van de Graaff, the plate counters under the direction of Mary Jones, and data analysis by Robert Lanier at Florida State University, the operating staff at the Los Alamos Omega West Reactor, John Palms who furnished the Ge detector, and the Danish Atomic Energy Commission and the staff at the reactor DR-3. The help of Mrs. K. H. Harper in drafting for this manuscript is gratefully acknowledged.